Preparation of Partially Graphitic Nanoporous Activated Carbon from Biomass and its Improving Electrochemical Performance of Supercapacitor

*Sivagaami Sundari Gunasekaran[a], Senthil Kumar Elumala1i[a], Thileep Kumar Kumaresan[a], Ramya Meganathan[a], Ashwini Ashok[a], Varsha Pawar[1,] , Kumaran Vediappan[c], Gnanamuthu Ramasamy [c], Smagul Zh. Karazhanov [d] Kalaivani Raman[*a,] , Raghu Subashchandra Bose[*b] ,*

[a]*Department of Chemistry, School of Basic Sciences, Vels University, Chennai -117.*

[b] *Vels Advanced Energy Research Centre, Vels University, Chennai -117.*

[c] *SRM University, Kattankulathur-603203*

[d]*Institute for Energy Technology, P.O Box 40, NO 2027-Kjeller, Norway.*

Corresponding Author Email: subraghu_0612@yahoo.co.in; rakvani@yahoo.co.in

Abstract

In this present work, the preparation of partially graphitic nanoporous carbon from biomass (bamboo bagasse) is carried out using potassium ferrocyanide and -KOH as activating agent with controlled temperature and gas flow rates. The physico-chemical properties of biomass-derived graphitic nano-porous carbon was characterized by X-ray diffraction studies, fourier transform infrared spectroscopy, thermal gravimetric analysis, raman spectroscopy, scanning electron microscopy, transmission electron microscopy and electrochemical measurements. It is interesting that the activation with the iron salts which acts as the catalyst plays a significant role in the formation of graphitic structures. The graphitic nanoporous carbonaceous materials show high specific surface area of 1360 m^2g^{-1}, low impedance, large pore volume and high specific capacitance. Thus, the iron-catalyzed graphitic carbon material is excellent candidate for the supercapacitor applications. This contemporary- novel method to synthesis of nanoporous carbon represents a great potential for apparent and diversified applications in energy storage materials.

Keywords: Graphene, Supercapacitor, Energy storage materials, Carbonization

Introduction

Supercapacitors/ultracapacitors/electrochemical capacitors play a vital role in energy storage technology by providing high power and cycling performances. Carbon-based materials are of interest because of their properties like high specific surface area, tunable porous structures and other distinguished properties. The most common form of carbon from the renewable energy is the biomass. Natural biomass-derived carbon has great attractive attention because of their interesting characteristics of naturally porous and heteroatom doping[4.] The use of biomass to produce energy is only one form of renewable energy that can be utilized to reduce the impact of energy production and use on the global environment. This green technology of deriving carbon from biomass can be applied over hue applications such as fuel cells, supercapacitors, water splitting devices with the use of electro-catalyst, lithium-ion batteries, etc.,

The major objective of this study is to prepare low cost, high conducting, and abundant electrodes for supercapacitor with stable cycling performances and also to synthesize partially graphitic nanoporous carbon from biomass. The current state of art in the field of supercapacitor is it has good power density, good reversibility and it is extensively used in high power applications such as grid applications, high power electronics, etc.. This study for the first time, is to overcome the above mentioned limitations by preparing the partially graphitic carbon which can be a synthetic graphene. This is a facile and easy method and the natural source is abundant, eco-friendly and low-cost. Thus, this would be extraordinary in the applications of supercapacitor[6].

Experimental

Carbonization and activation of bamboo bagasse

All chemicals used in this experiements are of analytical grade (AR). The physicochemical characterization of the material was carried out with thermal gravimetric analysis, x-ray diffraction studies, raman spectroscopy, fourier transform spectroscopy, scanning electron microscope (HitachiS-4800), transmission electron microscope and electrochemical measurements (Biologic SP300). The bamboo stick waste was broke into small pieces and weighed in a beaker. It was then treated into the muffle furnace (Hot King Instruments Company) at 300^0 C for almost 2 hours and cooled for 24 hours and thus the carbonized bamboo bagasse was obtained. The carbonized bamboo

bagasse was then homogeneously mixed and grinded with KOH (1:1) and mixture of KOH and + $K_3[Fe(CN)_6]$) in the ratio of 1:1:0.5.The powder was finely crushed and weighed in a boat crucible and kept into tubular furnace (BVN instruments Company)at different temperatures such as 600°C,700°C and 800°C for 2 hours, respectively with flow of inert gas atmosphere. Carbonization or activation is carried out and other traces of elements like oxygen, water, $-CH_2$ are completely burnt or vaporizes. It is then washed with HCl, hot water, and cold water for many times to neutralize in order to remove the impurities (KOH & other inorganic metals). It is then dried in vacuum oven at 120°C and hence KOH activated and KOH- iron catalyzed carbons are obtained, referred to as carbon and carbon-F.

For the three electrode system, the carbon and carbon-F was finely crushed and powdered. 90% of carbon, 10% of nafion solution (5%) which acts as a binder and required quantity of iso-propyl alcohol (IPA) is mixed homogeneously. It was then sonicated and made to stir for almost half an hour, until the solution gets fully dispersed. The prepared carbon and carbon-F were coated on the glassy carbon substrate (working electrode) and made to dry. The glassy-carbon electrode is used as the working electrode, the silver/silver chloride (Ag/AgCl) electrode is the reference electrode and the platinum wire electrode is employed as the counter electrode. The potassium hydroxide (6M KOH) serves as an electrolyte. The cyclic voltammetry was done for different scan rates within the voltage range of 0 to -1.0V. For full cell symmetric coin cell electrode system, the coin cell self-standing electrode is prepared, by homogenously mixing 85% of the prepared carbon and carbon-F, 5% Teflon and 10% conducting carbon (acetylene black). The paste is made into a film and it was made to dry in vacuum oven at 120^0C for 2 hours and the mass of the self-standing electrode is taken and are about 5-8 mg/electrode. The galvanostatic charge discharge experiments carried out within the voltage range of 0 to +1 under various current densities such as 1Ag-1 to 10Ag-1. .

Results and Discussion

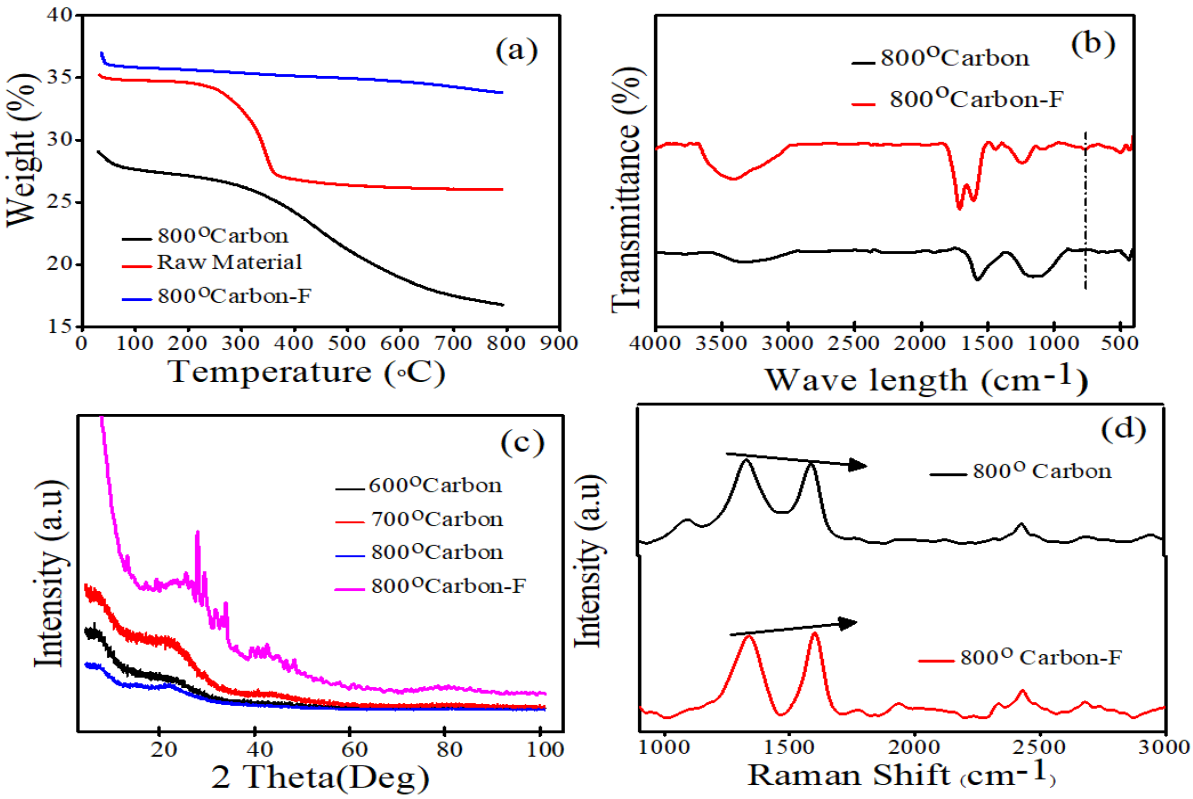

Figure 1: Representation of a) TGA b) FTIR c) XRD d) Raman Spectrum of carbon and carbon-F..

Fig(1a) represents the Thermal Gravimetric Analysis of the raw material, carbon and carbon-F . The TGA curves were taken in N_2 atmosphere at a heating rate of 15˚C/min The TGA curve of the raw material reveals that the decomposition (carbonization) starts from 260º. Hence, 300ºC was kept as the standard for the carbonization of the raw material. For 300 ºC carbonized materials, the activation appeared around 400ºC to 600 ºC and after that there is a linear decrease in the weight, thus few functional groups may be removed. For comparing 800 ºC activated carbon samples, the decomposition appear linearly and it is very stable. Hence, it indicates that there is a better removal of the functional groups. Figure (1b) illustrates the Fourier Transform Spectrum of carbon and carbon-F. The spectrum for the carbon shows the peak at 3381.57cm^{-1}, 1571.1 cm^{-1} and 1121.4 cm^{-1} which corresponds to a strong stretching mode of OH group, C=C stretching mode and stretching mode of C-O. And for the carbon-F, the peaks obtained are 3337.2 cm^{-1}, 1579.54 cm-1, 1160.94cm-1 and 436.798 cm^{-1} which corresponds to increases the stretching mode of C=C and decrease in the carbonyl group. These peaks (C=C) suggest that there is an increase in the graphitic nature while adding potassium hydroxide and potassium ferrocyanide mixture to the carbon. The carbon and carbon-F with different temperature (600ºC, 700ºC and 800ºC) was employed for the XRD studies. Figure (1c) corresponds to the XRD spectra of carbon and carbon-F of different temperature. Generally, for graphite the plane (002) will be 26.8 and plane (101/100) would be 43. The carbon has the two peaks at the plane (002) and (101) 22.3 and 43.The carbon-F shows two peaks at plane (002) and (101) at 25.8 and 43 which corresponds to the partial graphitic nature and its improved crystalline property. From these results, it is expected that, in presence of Fe salt catalyst and higher temperature to increases the graphitic nature of the porous carbon (i.e.) the amount of the catalyst and the graphitic nature of the carbon is thus directly proportional to each other. Figure (1d) corresponds to the raman spectra of carbon and carbon-F. This technique was employed because the analysis efficiently characterizes the carbon material as the raman scattering closely relates to the electronic structure of the materials. Here, the raman spectrum of the carbon shows D band at 1334$cm^{-1}$and G band peak 1597cm^{-1} respectively. The 2D peak is also found at 2431$cm^{-1}$and they are due to the resonant processes and it is the secondary peak. For comparison, the raman spectrum of the carbon- F shows D band at 1333cm^{-1} and G band peak 1591cm^{-1} respectively. The 2D peak is also found at 2433/cm and they are due to the resonant processes and it is the secondary peak. Hence, it can be concluded that the carbon-F has the partially graphitic nature. The carbon-F has increase in G band and has higher intensity than carbon. Thus the graphitic nature has been increased. The Id/Ig ratio of carbon and carbon-F was calculated and found to be 0.93 and 0.84 respectively, which represents the low graphitic crystalline structure.

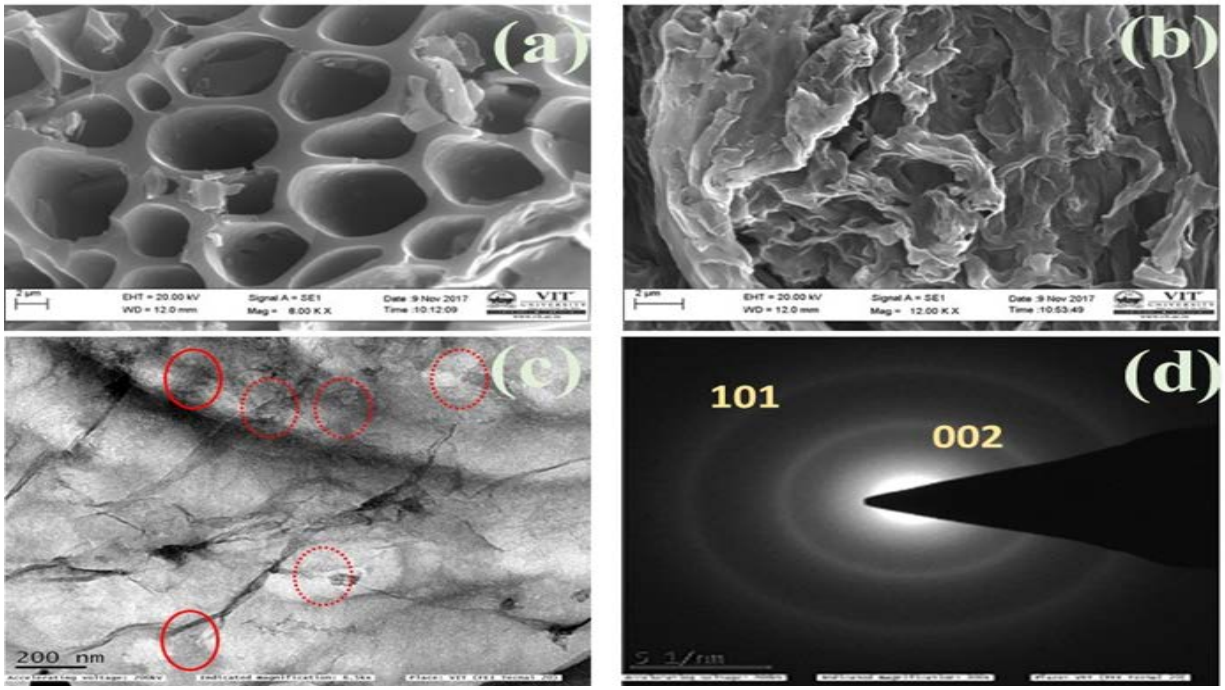

Figure 2: Representation of Figure 2. Representation of (a,b) scanning electron microscope (SEM) images carbon and carbon-F(c,d) Transmission Electron Microscope (TEM) image and SAED pattern of carbon-F.

Figure 2(a, b) represents low and high magnification of SEM micrographs of the carbon and carbon-F and it is very clear and confident from the figure that the carbon leads to the formation of hallow morphologies with more

micropores and the carbon-F has the morphology of paper like carbon nanosheets with porous cavities in sparse[8]. The TEM images (Fig 2c-d) represents the higher magnification TEM imaged and SAED pattern of carbon-F which shows the presence of pores in the 3D interconnected linked together in the carbon framework. This type of resemblance structure would be favorable and can be employed as an alternative electrode for the energy storage devices since it has been established the porosity and wrinkled morphology of the commercial graphene materials that governs its energy storage and power delivery capability.

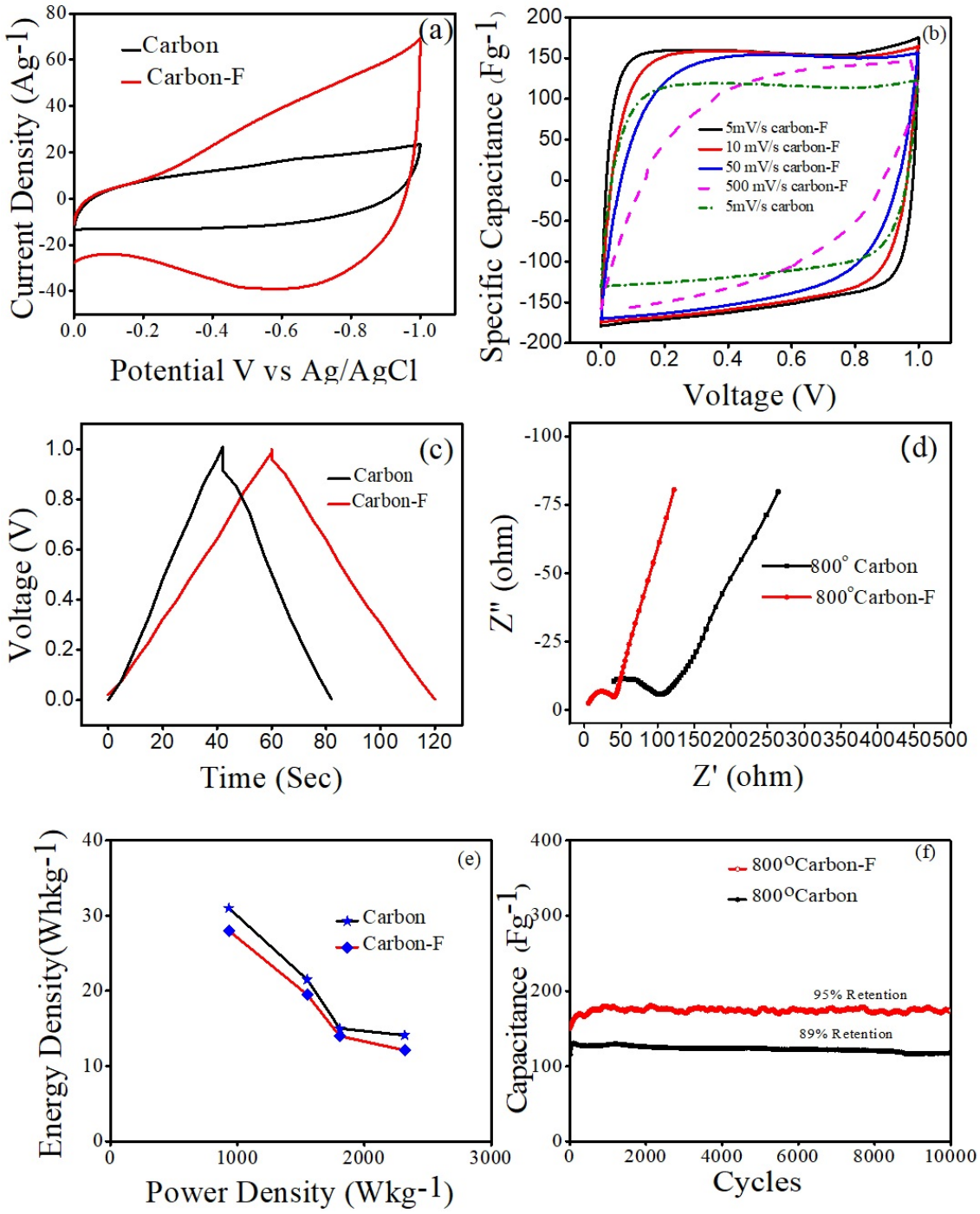

Figure 3 (a-f) represents the electrochemical measurements of the carbon and carbon-Ft.

The electrochemical studies involved the cyclic voltammetry, electrochemical impedance spectroscopy, Galvanostatic charge-discharge and cycling performances were done by Neware battery tester instrument. The symmetric devices were prepared with two electrodes separated by 0.18µm thick microfiber glass filter paper in CR2032 coin cells. The galvanostatic charge-discharge was performed in a potential window from 0 to 1 V at different current densities in 6 M KOH used as the electrolyte. The gravimetric specific capacitance for the electrode (C) F/g , energy density (E) Wh/Kg, powder density (P) W/Kg is calculated from the charge-discharge studies. The cyclic voltammetry study carried out at different negative scan rates (5,10,50,500 mV/s) . The voltage range applied for the studies is 0V to -1V and respectively. From the CV curve, the capacitance of carbon-F was calculated and found to be173. 22.9 F/g, 164 F/g, 156.0 F/g and 148 F/g respectively. For comparison capacitance of carbon was found to be 122 F/g at 10 mVs^{-1}. The shapes of all the CV curves was approximately rectangular and exhibits good symmetry even at higher scan rate, which indicates excellent capacitive behaviour and rate performances. Combining these results, it can be confirmed that the carbon-F approaches to the ideal condition of electrical double layer capacitor. The figure 3a-b,results shows, that carbon-F electrodes around 35 % higher capacitance, higher current densities $70Ag^{-1}$ and excellent electrochemical properties.

Figure (3C) represents the galvanostatic charge-discharge of the carbon and carbon-F at 1 Ag-1, 5Ag-1 and 10 Ag-1 were 174 Fg-1, 143Fg-1 and 128 Fg-1, respectively.. Obviously, the specific capacitance progressively decreases with increase in applied current density. In addition, overall current density of 1 to 10 Ag^{-1}, the specific capacitance decreases to 26 % of its initial value. Additionally, these results are comparable to those calculated from the CV curves, confirming the ultrahigh capacitance of the carbon-F electrode. Figure 3c shows the charge/discharge capacitance of carbon and carbon-F at a current density of 10A g^{-1}. It can be observed that the specific capacitance of carbon-F is much higher than that of carbon. The maximum specific capacitance of 128 Fg^{-1} was obtained at a current density of 10 Ag^{-1} for carbon-F and 114 Fg^{-1} for carbon respective

The Figure (3d) reveals the impedance spectroscopy of carbon and carbon-F. The electrochemical characterization was again studied by ohmic resistance of the electrode by the electrochemical impedance spectroscopy (EIS). The charge transfer of carbon-F was recorded by Nyquist plot and it shows their frequency range from 1Hz to 500KHz. The small semi-circle represents the fast charge transfer reaction, which leads to low resistance and high power density. The impedance of carbon and carbon-F is found to be 36Ω and 4 Ω. The distributed pore size in the structure can be identified by the elongated semicircle. At low frequency, EIS plot shows linearity, which in-turn the diffusion control of the electrode process under diffusion control can be studied. The slope of these lines are corresponding to the formation rate of the electric double layer (EDL). In general, it is confirmed that, shorter the slope, faster would be the EDL formed

Ragone's plot gives the relationship plot between relation energy density and power density of the symmetric capacitor. Figure (3e) depicts the Ragone's plot and the plot between specific capacitance and different current density. The energy density of carbon for-F 1A/g, 2 A/g, 5 A/g and 10 A/g is calculated as 12. 8. $WhKg^{-1}$, 12. 2 $WhKg^{-1,}$, 12. $1WhKg^{-1}$ and 12. 6 $WhKg^{-1,}$ respectively. The maximum energy density of 12. $8WhKhg^{-1}$ is obtained at 1A/g. The average current density is found to be 9.7 kWkg, 9.5 kWkg, 9.2 kWkg and 9. 2 kWkg respectively. The maximum power density of 2. 1 kWkg was obtained at higher current density of 10 A/g. Figure 3f reveals the cyclic performances of the as-prepared carbon and carbon-F at 10 Ag-1 for 10,000cycles. After the cell underwent 10,000 cycles, the capacitance retention of about 95% was obtained for carbon-F and for carbon the retention was 89%.. Thus, the retention corresponds the excellent long-term stability of the symmetric capacitor.

Conclusions

The biomass(bamboo stick waste) derived carbon was successfully prepared. Thus the carbon--F reveals the high specific capacitance and efficient rate capability for high-performance electro-chemical electrical double layer capacitor.. Generally, the natural biomass derived-iron catalyzed carbon is highly porous in nature. The biomass provides 10-14% of world's energy supply. The biomass derived carbon with iron as an activating agent has partial graphitic nature. The carbon-F reveals the average specific capacitance 148 F/g at 10A/g with stable cycling performance was obtained. This technology provides alternative graphene materials from biomass which would be a breakthrough in large-scale production. The carbon-F and carbon has 95% and 89% stable cycling respectively. Graphitic nature carbon reveals stable cycling and higher capacitance were found.

References:

1. Gaelle Guehenneux, Patrick Bussand, Meryl Brothier, Christian Poletiko, Guillaume Boissonnet, (2015) Fuel 84: 733-739, doi:/10.1016/j.fuel.2004.11.005

2. Wangla Tang, Yufan Zhang, Yu Zhong, Tong Shen, Xiuil Wang, Xinhul Xia, (2016) J.materresbull. doi:10.1016.

3. Peter McKendry, (2002), Bioresource Technology 83: 37-46.

4. Peter McKendry, (2002) Bioresource Technology 83: 47-54.

5. Jiang Deng, Mingming Li, Yong Wang (2016), , J.Green chemistry, doi:10.1039/C6GC01172A
6. Changping Ruan, Kelong Al, Lehul Lu (2014), , RSC Advances, doi:10.1039/C4RAD4470C.

7. Abdulhakeem Bello, Ncholu Manyala, Farshad Barzegar, Abubakar A.Khaleed, Damilola Y.Momodu, Julien K.Dangbegnon (2015), RSC Advances, doi:10.1039/C5RA2170BC.

8. Xi-Lin Wu, Tao Wen, Hong-Li Guo,Shubin Yang, Xiangke Wang, An-wu xu (2013), ACS Nano doi:10.1021/nn400566d.

9. Huanlei Wang, Zhi Li, David Mitlin (2013), ChemElectrochem-1: 332-337, doi:10.1002/celc.201300127.

10. A.Pozio, M.De Francesco, A.Cemmi, F.Cardellini, L.Giorgi (2002), , J.Power source 105:13-19. doi:10.1016/S03787753(01)00921-1.

11. Peter McKendry, (2002
12. Demirbas A (2001), , Fuel 80:1885-91. doi:10.1.1.925.2983

13. Morf.P, Hasler.P, Nussbaumer.T (2002), Fuel process Technology 75:27-43. doi:10.1002/anie.201205545

14. Guehenneux G, Varin.S, Le T.T.H, Baussand.P (2003), Grenoble. doi:10.1016/j.fuel.2016.01.051

15. Liang H.w, Guan Q.F, Chen L.F, Zhu Z, Zhang W.J, Yu S.H, (2012), , Angew.Chem, Int.Ed 51:5101-5105. doi.:10.1016/j.fuel.2016.01.051

16. White R.J, Budarin V, Luque R, Clark J.H, Macquarrie D.J (2009), Chem.Soc.Rev 38: 3401-3418. doi:0.1039/b822668g

17. Seliktar D (2012), , Science 336: 1124-1128. doi.:10.1126/science.1214804.

18. Li J, Liu C.Y, Liu Y (2012), J.Mater.Chem 22: 8426-843c0. doi:10.1039/C2JM16386A.

19. Chen J, Sheng K, Luo P, Li C, Shi G (2012), Graphene hydrogels deposited in nickel foams for high rate electrochemical capacitor, Adv.Mater 24: 4569-4573. doi:10.1002/adma.201201978

20. Xu Y, Shen K, Li C, Shi G (2010), , ACS Nano 4: 4324-4330. doi.:10.1021/nn10187z.

21. Titirici M.M, Antonietti M (2010), , Chem.Soc.Rev 39: 103-116. doi:10.1039/B819318P.

22. Chen L.F, Zhang X.D, Liang H.W, Kong M, Guan Q.F, Chen P, Wu Z.Y, Yu S.H (2012), , ACS Nano 6: 7092-7102. doi/10.1007/s12274-016-114.